A Low Cost, Sensor-less Drag Force Estimation Methodology via Measuring of Motor Currents

Vassilios Tsounis, *Member, IEEE*, Michail Makrodimitris, *Student Member, IEEE*
and Evangelos Papadopoulos, *Senior Member, IEEE*

***Abstract*— Modeling and control of underwater vehicles presents the challenge of sufficiently identifying acting hydrodynamic forces. Modern approaches assume the use of direct sensor measurements, which usually involves expensive and complicated set-ups. In this paper, a new approach to estimating hydrodynamic drag forces is proposed that does not employ a force sensor. The developed methodology involves processing the system responses and motor current measurements. A low cost towing carriage system is developed, driven by a 2-axis servomechanism with composite chains, off-the-shelf electronics and custom software running on the BeagleBone embedded platform. The sensor-less methods are described and the resulting drag estimates are experimentally compared to measurements produced by a 6-DOF force sensor, showing the merits of the developed methods.**

***Index terms*— Drag Force Estimation, Sensor-less Force Estimation, Multi-axis Motion Control, Tow-tank System, Model Identification.**

I. Introduction

Measurement of hydrodynamic forces acting on submerged bodies is important when developing the system's dynamical model. This is especially important for achieving accurate motion control in underwater robotics and thus has been a subject of extensive research in the control theory and robotics fields spanning the last two decades. Hydrodynamic drag forces specifically, are important for the design of the necessary propulsion system for achieving accurate tracking of desired trajectories in aquatic environments. Additionally, knowing the drag forces also helps in estimating the power requirements of target trajectories, thereby aiding system autonomy. Methods for measuring drag forces vary greatly and many distinct approaches exist in the literature such as Planar Motion Mechanisms (PMMs), system identification methods, state observers, simulations based on Computational Fluid Dynamics (CFD), wind tunnel and inertial or direct force measurements.

Wind tunnels can be used to measure wind resistance which could be used to compute the respective drag in water by equating the Reynolds numbers of the two media, [1]. This may result in high uncertainty in certain cases where dynamic and kinematic similarity is not fulfilled simultaneously. Velocity measurements such as Particle Image Velocimetry (PIV) or Hot-Wire Anemometry, apply the conservation of momentum to calculate the effective forces acting on the moving body, [2]. Extensive research focusing on CFD software simulation techniques, has also proven useful in providing non-experimental methods for calculating drag [3]. In naval engineering, it is common to use PMMs to rigorously collect steady-state and transient speed data of scaled models in a tow-tank plus force sensor configuration such as the one shown in Fig. 1a, [4]. The aforementioned approaches usually are expensive because either commercial software licenses and/or costly equipment are required. Simpler methods which use basic physical principles such as standard weights and pulleys to conduct falling-time and speed measurements are conducted in [5] to estimate drag coefficients and added mass. However, several arduous experiments are needed in methods such as these.

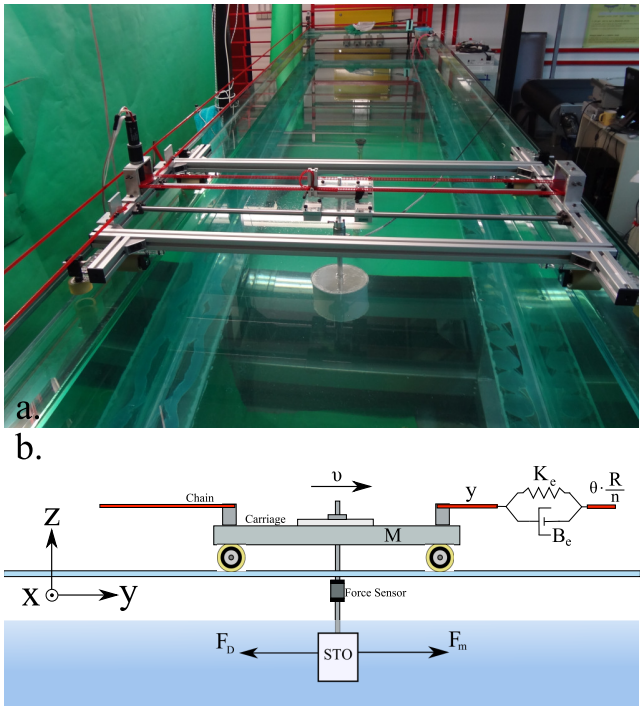

Figure 1. (a) Tow-tank carriage servomechanism, (b) free-body diagram of system dynamics.

Other methods for estimating drag forces use System Identification (SI) algorithms. SI approaches provide means for estimating - both online and offline - parameters of assumed model structure by applying known excitations and

Vassilios Tsounis is student at the School of Electrical and Computer Engineering, Michail Makrodimitris and Evangelos Papadopoulos are with the Department of Mechanical Engineering, National Technical University of Athens (NTUA), Greece (phone: +30-210-772-2643, 1440; fax: +30-210-772-1450; e-mail: vastsoun@gmail.com , mmakrod@mail.ntua.gr, egpapado@central.ntua.gr,).

collecting response data. These usually include Linear and Nonlinear Observers (Kalman filters, Nonlinear Disturbance Observers etc.) [6], [7]. However, these approaches when applied to underwater systems would require Inertial Measurement Units (IMUs) or external equipment such as cameras to measure the state of the system.

Unrelated though to the previous, works exist within the literature where electrical measurements on motors are used to estimate forces, [8], [9], [10]. This motivates the interesting question of whether certain hydrodynamic forces can be measured -at least indirectly- by using very simple means; measuring the current of a motor which drives an object across a water tank. This work aims to show that for certain applications in robotics and control, if a tow-tank setup or something similar is available, then it could be used for identifying hydrodynamic drag forces acting on the submersible without the need for expensive force sensors or IMUs. In this paper, we present a novel methodology for measuring drag forces through the processing of system response and motor current signals. The first method proposed involves executing a particular maneuver twice and then processing the motor current signals. The second utilizes a model of the servomechanism to predict the presence of drag needing only a single execution of any maneuver but is cumbersome due to the need for executing identification experiments beforehand. Provided though that a model of the system is available, the same data set may then be used in conjunction with SI methods, when online real-time estimates may also be desired. The proposed methods are then compared to directly using a force sensor. The experimental set-up employed in this paper was realized by designing and implementing a Cartesian multi-axis servomechanism, moving over a parallelepiped reinforced glass water tank which serves as the primary test-bed for the Control Systems Lab's (CSL-EP, NTUA) robotic fish.

II. Towing Carriage Design and Implementation

A. Mechanical Design

A towing carriage system, see Fig. 1, was designed and constructed to support research in underwater robotics and specifically experiments centred on NTUA-CSL's robotic fish. The primary design requirements included the overall cost, the operational bandwidth appropriate for the maneuvering with the robotic fish, the low power, modularity and extendibility as well as considerations for the work environment.

Although for Cartesian servomechanisms it is most common to use belt drives or ball-screws, the decision was made to avoid these. Due to the 5m length of the tank along the larger axis, belts would be impractical, while ball-screws would be too heavy (i.e. stresses on the glass tank structure) and very expensive. Plastic chains reinforced with steel wire pose a viable alternative, as they are not prone to slip like belts while being more durable and just as inexpensive. Rollers with ball bearings provide planar motion in the main y (long) axis, while linear shaft bearings are used for the secondary x (short) axis. Both are less stiff than ball-screws, therefore lowering the power requirements on the choice of actuator motors. Another property resulting from the choice of elastic chains, and important considering the laboratory environment, is that it is virtually soundless. In fact, most of the sound is produced by the motor transmissions and driver amplifiers.

The base frame and motor mounts are constructed with aluminium components in a simple arrangement. For these, off the shelf struts with linear slide rails where used, in combination with several steel elements like the sprockets, shafts, rollers and the ball bearings. For both x and y axes, the same kinematic configuration of motor-coupler-sprocket-chain was used. The larger y axis drives the orthogonal base frame, within which, the x axis drives the End-Effector Platform (EEP) over linear shaft bearings. The EEP can accommodate several sensor mounts as well as a third orientation axis, for the specific experiments of this paper though, a force sensor is mounted between the EEP and the Submerged Test Object (STO). This configuration results in a coupled two mass system where the hydrodynamic drag forces acting on the STO, load the total y axis dynamics. Fig. 1b shows the system configuration.

B. Electronics Design

Regarding actuation, two permanent magnet brushed Maxon DC (PMDC) motors were selected, with 60W and 20W power ratings for the long and short axis respectively. Each motor is equipped with an incremental encoder with 1000 lines per revolution. This resolution is effectively quadrupled through the decoding of the quadrature signals. Each motor includes a 35:1 planetary gearbox with their output shafts coupled to the chain sprockets via elastic aluminium shaft couplers. PMDC motors provide simple means of actuation, as they do not require complicated power electronics to be driven. As such, two Maxon ADS 50V/5A four-quadrant motor drives were chosen to drive the motors in current-control mode thus enabling direct control of the motor torques.

A waterproof 6-Dof ATI Nano25 Force Sensor was used to directly measure the acting drag forces and serves as a benchmark for the methods presented in this work. The sensing range of the force sensor is within [0,125] N, along the x and y axes, see Fig. 1. The resolution is about 1/48 N. Additionally, the accompanying software provides data sampling rates of up to 10 kHz.

C. Control Electronics

In the same spirit of low cost design, an effort was made to avoid the need for expensive industrial control electronics. The final decision was to use the BeagleBone open-hardware embedded platform as it provides very attractive capabilities in regard to its use in motion control/robotic systems. This platform is built around the AM3359 SoC IC from Texas Instruments (TI), which is based on a cortex-A8 32-bit ARM processor with hardware floating-point capabilities. Also, it has a very expansive set of peripheral modules (all within the single IC unit) that support popular digital and analog input-output forms. All IO signals are accessible from the BeagleBone's two, multiplexed pin-out headers.

In order to interface the modules to the magnetic incremental encoders mounted onto the motors, and the ADS motor drives, a custom system using widely available electronics commonly found in industry, was designed and built. For realizing real-time motion control, the need for precise and deterministic control loops is exceptionally critical. While the BeagleBone is intended as a Linux platform, the previous requirement combined with the overhead of the OS, drove the decision to write custom software based on the StarterWare open-source firmware package available from TI. The source code, written in C, was compiled with an embedded GCC toolchain from CodeSourcery. The resulting real-time control system is capable of implementing a control loop for all the actuators, sensors and algorithms, with a frequency of up to 4 kHz.

III. System Dynamics & Control

In this section we will describe the hydrodynamic forces acting on the STO during motion, models for the tow-tank carriage system, a controller for executing the experiment trajectories and the methods for measuring and estimating the acting drag forces.

A. Hydrodynamic Drag

The scope of this paper is identifying drag forces acting on submerged bodies to enable future work on model based controllers for robotic fish. These controllers need to predict the acting drag forces, to a certain degree of accuracy, in order to improve trajectory tracking performance. The model assumed for these forces is that of viscous drag proportional to the square of velocity υ:

$$F_D = \frac{1}{2}\rho \upsilon^2 C_D A \tag{1}$$

Where ρ is water density, C_D is the drag coefficient and A is the surface area of the cross section exposed to the flow. Even though (1) applies for a body of any geometry, our focus is on comparing experimental measurements and so in order to simplify the setup an object of simple geometry was chosen to conduct experiments. A plastic cylinder of radius $R_{cylinder} = 10cm$ and height $H_{cylinder} = 20cm$ was used as the STO. A simplified form of the previous equation, for the purpose of drag identification, is the following:

$$F_D = D_d \upsilon^2 \tag{2}$$

Where D_d is in Ns^2/m^2 units. Using a Least Squares (LS) computation over the values of steady-state speeds and respective forces measured, the effective coefficient D_d that multiplies υ^2 can be calculated.

B. Tow-tank Carriage System

As is common in Cartesian servomechanisms, the mechanical design permits the use of configurations where the coupling forces between axes of motion can be made negligible. This enables the modeling and control of each axis to be independent of the others. Also, since the specific carriage servomechanism uses the same drive configuration for both axes of motion, this permits us to reuse the same model structure for both axes, with a difference only in the set of model parameter values. This modular configuration consists of a motor-gearbox set coupled to the shaft of the first sprocket in a sprocket pair. The sprocket pair is driven by the plastic reinforced chain with the ends mounted onto the target platform. For the y axis, this target is the base frame of the carriage, while for the x axis, it is the EEP.

During initial testing of this configuration, it was observed that each axis did not exhibit simple dynamics during motion. Both, but especially the longer y axis, exhibited transient oscillations in the speed and acceleration responses when sudden excitations such as step inputs where applied. It was evident that a model of higher order would be required in order to account for the oscillations. The system model that was most successful in recreating the observed transient behavior is that of the following:

$$J_m\ddot{\theta} + B_m\dot{\theta} + C_m sign(\dot{\theta}) - K_e\frac{R}{n}\left(y - \frac{R}{n}\theta\right) - B_e\frac{R}{n}\left(\dot{y} - \frac{R}{n}\dot{\theta}\right) = \tau_m \tag{2a}$$

$$M\ddot{y} + B\dot{y} + Csign(\dot{y}) + K_e\left(y - \frac{R}{n}\theta\right) + B_e\left(\dot{y} - \frac{R}{n}\dot{\theta}\right) = 0 \tag{2b}$$

The system parameters are given in Table I.

TABLE I
System Model Parameters

Quantity	Symbol	Units
Motor Inertia	J_1	Kgm^2
Carriage Mass	M_2	Kg
Viscous Friction Coeff.	B_1 , B_2	Ns
Coulomb Friction	C_1 , C_2	Nm
Elasticity Stiffness	K_e	N/m
Elasticity Damping	B_e	Ns
Gearbox Ratio	n	-
Sprocket Radius	R	m
Motor Torque	τ_m	Nm

Equations (2) are is derived from a Lagrangian formulation assuming that the vibrations can be accounted for by using a spring-damper pair, existing between the motor sprocket and the EEP, to model the behavior of the chain. The motor side angle of rotation is θ and the EEP position is noted by y. Equation (2) is of the form commonly employed to describe systems with joint elasticity, [11]. Experiments showed that a dominant frequency mode existed for each axis; $\simeq 13Hz$ in the y axis and $\simeq 45Hz$ in the x axis. As described in [11], these types of systems exhibit dynamics on two time scales. The previous frequencies are modes of the transient oscillations of the fast-time scale dynamics. This behavior becomes significant during large accelerations resulting in relative motion between carriage and motor. This motion could not

be measured since there was no equipment available to measure the ground truth state of the EEP in either axis. Therefore, identifying the model parameters of the underlying slow-time scale dynamics was a major challenge. However, smooth trajectories (i.e. acceleration is continuous function) can guarantee that the fast-time scale dynamics are not excited and so for our purposes we need only describe the slow-time scale dynamics, to which the system asymptotically converges, as is shown in (3):

$$J_{eff}\ddot{\theta} + B_{eff}\dot{\theta} + C_{eff}\,sign\left(\dot{\theta}\right) = \tau_m,\ \theta \approx \frac{n}{R}y \qquad (3a)$$

Where:

$$J_{eff} = J_m + M\cdot\frac{R^2}{n^2}, B_{eff} = B_m + B\cdot\frac{R^2}{n^2}, C_{eq} = C_m + C\cdot\frac{R}{n} \qquad (3b)$$

Since current control is used to drive the motors, then the following relations are also considered:

$$\tau_m = K_T i_m = K_T K_{amp} v_c \qquad (4)$$

K_T is the motor torque constant, and K_{amp} is the current control gain of the motor driver amplifier that produces an armature current proportional to the control voltage signal v_c from the BeagleBone and interface system. The parameters for this system are also given in Table I. Equation (3a) describes the effective dynamics for each axis of the carriage system. The respective parameters are the ones to be identified experimentally, as described in the following section.

C. Model Parameter Identification

Since equation (3a) is linear with respect to the unknown parameters, the Ordinary Least Squares (OLS) algorithm, see [12], was used to identify the parameters of the effective system:

$$\hat{\theta}_{OLS} = \left(\Phi^{\mathrm{T}}\Phi\right)^{-1}\Phi^{\mathrm{T}}\tau_m \qquad (5)$$

Where,

$$\hat{\theta}_{OLS} = \begin{bmatrix}\hat{J}_{eff}\\ \hat{B}_{eff}\\ \hat{C}_{eff}\end{bmatrix}^T, \Phi = \begin{bmatrix}\ddot{\theta}_0 & \dot{\theta}_0 & sign(\dot{\theta}_0)\\ \vdots & \vdots & \vdots\\ \ddot{\theta}_N & \dot{\theta}_N & sign(\dot{\theta}_N)\end{bmatrix}, \tau_m = K_T K_{amp}\begin{bmatrix}v_{c,0}\\ \vdots\\ v_{c,\mathrm{N}}\end{bmatrix}$$

Where N is the total number of time steps in the data set. The sought values are that of the dynamic parameters of the effective system (3).

To ensure convergence of this computation to valid model parameters, certain caveats of using this algorithm must be addressed. Firstly, an appropriate excitation must be used in order to produce response data that contains most if not all of the behavior of the system. A series of square pulses was selected for the excitation of the y axis. The final requirement on the open-loop procedure was that of a data set of significant size, in order to ensure convergence close to the parameter values. The resulting response signals are then filtered using a Gaussian smoothing curve, so that noise and oscillation components were significantly reduced.

D. Controller Design

For measuring drag forces assuming the model of (2), it is necessary that the carriage and carriage-coupled-STO systems achieve steady-state velocities in the y axis with a sufficient degree of accuracy. Steady state speed trajectories are realized by tracking trapezoidal speed profiles. The executed trajectories must be of this form, in order to avoid transient effects such as added mass and the disturbances induced from turbulent flows. These would cause the deterioration of the force measurement accuracy.

PID control is employed in order to achieve the desired trajectories with sufficiently small tracking errors. These controllers are simple, straightforward to implement and can be used without the need for a system model. Primary motivation for resorting to these is that this work aims to evaluate the possibility of employing simple controllers to measure drag forces, treating them as general disturbances.

$$v_c = K_P(\theta_d - \theta) + K_D(\dot{\theta}_d - \dot{\theta}) + K_I\int(\theta_d - \theta)dt \qquad (6)$$

The Ziegler-Nichols gain tuning method [13] was used in order to obtain initial gain values. These were then further tuned empirically to achieve stiff control loops which would ensure that the desired trajectory values were maintained. Specifically, the longer y axis used a complete set of PID gains to minimize the tracking error and achieve sub-millimeter accuracy. The values of the PID controller gains are given in Table II.

E. Drag Estimation Methods

As mentioned earlier, the carriage system currently is capable of 2-DOF planar motion and is extendable to a third rotation θ_{xy} in the x-y plane. We focus on showing that drag forces are measurable in a single DOF linear motion. Three methods are proposed and compared in order to measure the acting hydrodynamic forces. The first is a direct measurement using the ATI force sensor, while the other two constitute the estimation methods and are executed over the same data set which results from precisely repeated trapezoidal speed profiles along the y axis. In each procedure, data is collected while the carriage tows a simple cylindrical STO. Let $f(\theta,\dot{\theta},t)$ be the function representing the total loading torque on the y axis motor without the presence of hydrodynamic forces. If this system is in steady-state with constant speed, this becomes $f_{ss}(\theta,\dot{\theta},t)$ and when drag forces are present, the torque balance equation becomes:

$$f_{ss}(\theta,\dot{\theta},t) + \frac{R}{n}F_D = K_T K_{amp} v_c \qquad (7)$$

The proposed drag estimation methods are described as follows:

Method 1: Using a Force Sensor.

As is shown in Fig. 1b, the object, whose drag force is to be estimated, is mechanically coupled to the towing carriage, with the force sensor placed exactly in between. The drag force is then effectively the force F_y, measured by the force

sensor along the long tank axis during the steady-state phase of the trapezoidal profile executed by the controller. These Force Sensor Method (FSM) measurements however are conducted during all iterations of the experiments, including those of the estimation methods, so as to provide a benchmark for their performance.

Method 2: Two-Step Motor Current Measurements.

Assuming no previous knowledge of the plant model or system parameters, a PID control law can be applied. If the gains are appropriately chosen in order to ensure stiff trajectory tracking, then executing any same procedure twice, the first with the STO mounted below the EEP and in the water (input $v_{c,1}$), while in the second, mounted on top of the EEP (input $v_{c,2}$). By then taking the difference between (6) from each experiment, i.e. the Motor Current Difference (MCD), this should yield the drag force signal:

$$F_{\mathrm{D}} = \frac{n}{R} K_T K_{amp} (v_{c,1} - v_{c,2}) \tag{8}$$

Method 3: Single-Step Model Based Estimation.

This is the Model Based Drag Prediction (MBDP) method and considers the use of (7) and the model (3) in place of $f(\theta, \dot{\theta}, t)$ for the y axis dynamics. Using the parameters of Table II, we proceed to predict the total forces produced only by the carriage system, which are then subtracted from the known input control torque. Even though this signal is also affected by other hydrodynamic forces during transient motion, these are negligible during steady-state. In this case, the drag force can be estimated through the following calculation:

$$F_{\mathrm{D}} = \frac{n}{R} (K_T K_{amp} v_c - J_{eff} \ddot{\theta} - B_{eff} \dot{\theta} - C_{eff} sign(\dot{\theta})) \tag{9}$$

IV. EXPERIMENTAL RESULTS

A. Carriage Parameter Identification

TABLE II
EFFECTIVE SYSTEM PARAMETERS

Quantity	SYMBOL	Value
Effective Inertia	J_{eff}	1.502e-5 kgm^2
Effective Viscous Friction	B_{eff}	4.657e-6 Ns
Coulomb Friction	C_{eff}	3.9e-3 Nm
Torque Constant	K_T	26.7e-3 N/m
Amplifier Gain	K_{amp}	0.352 A/V
Gearbox Ratio	n	34.97
Sprocket Radius	R	5.5 cm
P Gain	K_P	1.32e-6
I Gain	K_I	3.29e-10
D gain	K_D	1.32e-7

The OLS identification method was used, following the experimental procedure, which was executed with an input signal consisting of a series of square pulses of 60% duty and a period of $1\mathrm{sec}$. The resulting parameter values are listed at the top of Table II.

B. Drag Experiments

Following the aforementioned methods in the previous section, a set of trapezoidal speed profiles were carried out along the y axis of the carriage tank. The x axis was controlled so to remain centered in the middle of the tank's width. The symmetrical trapezoid profiles covered distances of up to $2.2m$, at steady-state speeds between $5cm/s$ and $55cm/s$ with $10cm/s$ increments, accelerating to the target velocity within less of a second. The profiles where modified appropriately so as to avoid excitation of the oscillation modes. The tracking errors of the desired trajectories (position and velocity) are shown in Table III, for both cases, i.e. with and without drag. It is clear that the controller achieves the desired trajectory with a sufficient degree of repeatability and accuracy. The errors are calculated from the raw values of the encoder i.e. they have not been filtered to remove noise and/or other disturbances.

TABLE III
TRAPEZOID EXPERIMENT TRAJECTORIES

Steady-state Velocity (mm/s)	Mean Position Error (mm)	Mean Velocity Error (mm/s)
50	3.36e-1	1.69e-2
150	5.81e-1	6.9e-2
250	8.17e-1	9.87e-2
350	1.8	3.8e-2
450	1.9	1.63e-2
550	3.9	2.31e-2

C. Method Comparison & Discussion

Subsequently, having assured that responses are practically identical to command, we present the results of using the sensor-less drag estimation methods and compare their performance to that of the force sensor. These are presented in Table IV and the identified drag force curve, plotted against velocity are shown in Fig. 2.

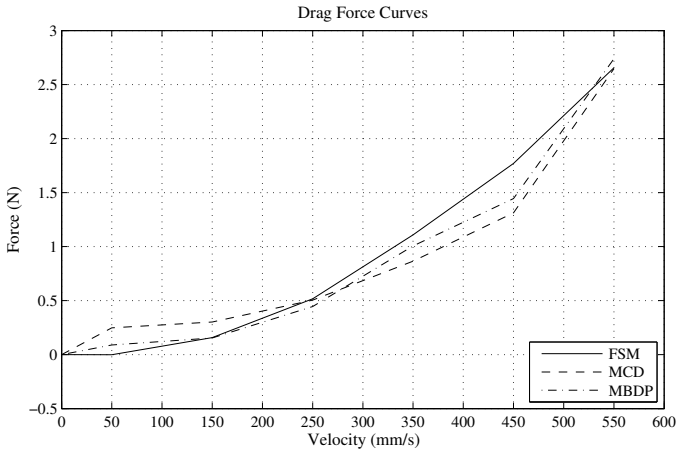

Figure 2. Measurements of the force sensor during trapezoidal motion.

From Fig. 2 it is clear that the method using differences in motor current produces results significantly closer to those by the FSM than to those by the MBDP method. The coefficients of drag which were identified via LS are also shown and compared in Table IV with the results of the fitting.

TABLE IV
D_d - DRAG COEFFICIENT COMPARISON

ATI Force Sensor (FSM)	Motor Current Difference (MCD)	Model Based Drag Prediction (MBDP)
8.78e-2 Ns^2/m	8.4e-2 Ns^2/m	7.87e-2 Ns^2/m

A force comparable to that of the FSM is detected in both estimation methods. However, the estimations deviated from the sensor measurements during the acceleration and deceleration phases. This was expected since transient responses are also affected by additional hydrodynamic effects such as added mass. During the course of conducting identification experiments, it was observed (see Fig. 3, $t \geq 2.5\,\text{sec}$) that the loading forces increased as the carriage traversed the middle of the tank. This dependence on position was not accounted for in the system model, therefore significantly contributing to the deviation of the model based approach from the results of the other methods. Also, a deviation of about $\pm 0.2N$ was observed in the FSM measurements and was detected by checking the sensor's output using standardized weights. This though, is most likely attributed to thermal effects.

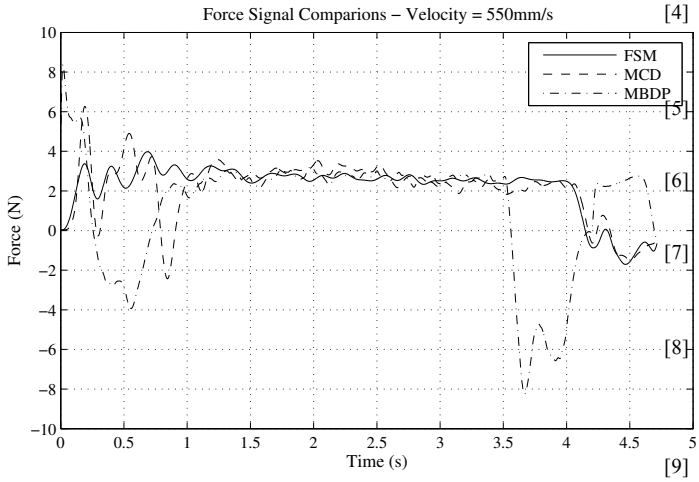

Figure 3. Measurements of the force sensor during trapezoidal.

CONCLUSIONS

In this paper, we presented a new approach for estimating drag forces without the use of a force sensor. Force estimation was realized with two methods and compared with the direct FSM measurements. The first method consisted of comparing the motor currents assuming identical trajectories where executed; with and without the presence of drag. The second relied on an identified system model for the tow-tank carriage to predict the disturbance from known inputs and responses. This work has demonstrated the validity of the sensor-less approach, as the identified drag coefficient is in good agreement with the value produced by the force sensor.

FUTURE WORK

Continuations of the work presented in this paper intend to develop a more accurate model of the carriage dynamics to account for the system's flexibilities and therefore provide an improved MBDP method. This requires an exterior sensor system to be implemented in order to measure the end-effector platform's ground-truth trajectory. Furthermore, the procedures described here are to be tested in a 3DOF system with complete planar motion (also with planar rotation) and conducted on the robotic fish.

ACKNOWLEDGMENTS

The authors would like to thank Klajd Lika, K. Koutsoukis and K. Mahairas for their help with the setting up and execution of the experiments.

REFERENCES

[1] Papadopoulos E., Apostolopoulos E., and Tsigkourakos P., "Design, control, and experimental performance of a teleoperated robotic fish," *IEEE 17th Mediterranean Conference on Control and Automation, 2009 (MED '09)*, 24-26 June 2009, pp.766-771.

[2] D. F. Kurtulus, F. Scarano, L. David, "Unsteady aerodynamic forces estimation on a square cylinder by TR-PIV", *Journal of Experiments in Fluids*, February 2007, Volume 42, Issue 2, pp 185-196.

[3] Gerasimos K. Politis, Application of a BEM time stepping algorithm in understanding complex unsteady propulsion hydrodynamic phenomena, *Journal of Ocean Engineering*, Volume 38, Issue 4, March 2011, Pages 699-711.

[4] Shea, D., Williams, C., Moqin He, Crocker, P., Riggs, N., Bachmayer, R., "Design and testing of the Marport SQX-500 Twin-Pod AUV," *Autonomous Underwater Vehicles (AUV), 2010 IEEE/OES* , vol., no., pp.1-9, 1-3 Sept. 2010

[5] Wei Leung Chan and Taesam Kang, "Simultaneously Determination of Drag Coefficient and Added Mass" *IEEE Journal of Oceanic Engineering*, Volume: 36, Issue: 3, 2011 pp. 422-430.

[6] A. Gupta and O'Malley, M. K., "Disturbance observer-based force estimation for haptic feedback", *ASME Journal of Dynamic Systems, Measurement and Control*, vol. 133, pp. 014505-1--014505-4, 2010.

[7] Sang-Chul Lee; Hyo-Sung Ahn, "Sensorless torque estimation using adaptive Kalman filter and disturbance estimator," Mechatronics and Embedded Systems and Applications (MESA), 2010 IEEE/ASME International Conference on , vol., no., pp.87,92, 15-17 July 2010

[8] Linderoth, M.; Stolt, A.; Robertsson, A.; Johansson, R., "Robotic force estimation using motor torques and modeling of low velocity friction disturbances," Intelligent Robots and Systems (IROS), 2013 IEEE/RSJ International Conference on , vol., no., pp.3550,3556, 3-7 Nov. 2013

[9] Xiaoli Li, "Development of current sensor for cutting force measurement in turning," *IEEE Transactions on Instrumentation and Measurement,* , vol.54, no.1, pp.289,296, Feb. 2005.

[10] Ronkanen, P., Kallio, P., Koivo, H.N., "Simultaneous Actuation and Force Estimation Using Piezoelectric Actuators," *International Conference on Mechatronics and Automation, 2007, (ICMA 2007),* vol., no., pp.3261,3265, 5-8 Aug. 2007.

[11] Petar Kokotovic, Hassan K. Khalil and John O'Reilly, *Singular Perturbation Methods in Control: Analysis and Design*, Classics in Applied Mathematics, Reprint edition 1987.

[12] Lennart Ljung, *System Identification: Theory for the User*, Prentice Hall, 2nd Edition, 1999.

[13] Karl Karl Johan Åström, Tore Hägglund, *Advanced PID Control, ISA-The Instrumentation, Systems, and Automation Society, 2006.*